Preparation of Chitin Nanofibers by Surface Esterification of Chitin with Maleic Anhydride and Mechanical Treatment

Yihun Fantahun Aklog[a], Tomone Nagae[a], Hironori Izawa[a], Minoru Morimoto[b], Hiroyuki Saimoto[a], Shinsuke Ifuku[a,*]

[a] Department of Chemistry and Biotechnology, Tottori University, 4-101 Koyama-minami, Tottori 680-8552, Japan

[b] Research Center for Bioscience and Technology, Tottori University, 4-101 Koyama-minami, Tottori 680-8553, Japan

*Corresponding author: Department of Chemistry and Biotechnology, Tottori University, 4-101 Koyama-cho Minami, Tottori 680-8550, Japan. Tel and Fax: +81-857-31-5592, e-mail: sifuku@chem.tottori-u.ac.jp

ABSTRACT

Esterification with maleic anhydride significantly improved the mechanical disintegration of chitin into uniform 10-nm nanofibers. Nanofibers with 0.25 degrees of esterification were homogeneously dispersed in basic water due to the carboxylate salt on the surface. Esterification proceeded on the surface and did not affect the relative crystallinity. A cast film of the esterified chitin nanofibers was highly transparent, since the film was free from light scattering.

Keywords: Chitin; Nanofiber; Esterification with maleic anhydride

1. Introduction

A nanofiber is defined as a fiber with a diameter of less than 100 nm. Due to their unique morphology, nanofibers are quite different from micron-sized fibers in their dimensional, optical, and mechanical properties. Chitin is the second most abundant biopolymer on earth that has *N*-acetyl glucosamine repeating units, and is the main component of exoskeletons of crustaceans such as crab and prawn. An exoskeleton has a hierarchical structure consisting of fine chitin nanofibers (Raabe et al., 2006; Chen et al., 2008). Recently, chitin nanofibers were obtained by the mechanical

disintegration of commercial chitin powder extracted from the shell of red snow crab (Ifuku et al., 2010). The nanofibers were highly uniform, with widths of approximately 10 nm. Since commercial chitin powder consists of aggregates of nanofiber, chitin was transformed into nanofibers by mechanical processing (e.g., high-pressure fluidizing (Kose et al., 2011; Ifuku et al., 2012; Ajoy et al., 2013), disk milling (Ifuku et al. 2009; Ifuku et al., 2011), and ultrasonic breaking (Fan et al., 2008b; Fan et al., 2012; Lu et al., 2013), powerful blender (Mushi et al., 2014; Mushi et al., 2016). However, strong mechanical stress was required to disintegrate chitin into nanofibers due to the strong hydrogen bonding generated between nanofibers. A lot of energy was consumed to obtain nanofibers, raising their production cost. Thus, the development of an efficient disintegration process is indispensable to the commercial application of chitin nanofibers.

Chemical treatment can improve disintegration efficiency. For instance, Isogai et al. reported chitin nanocrystals prepared by TEMPO-mediated oxidation of α-chitin (Fan et al., 2008a). Carboxylate groups were formed by the oxidation of chitin at the C-6 primary hydroxyl group on the nanofiber surface, facilitating mechanical disintegration with the assistance of the osmotic pressure effect. Iwamoto et al. prepared lignocellulose nanofibers by the esterification of wood flour with maleic anhydride (Iwamoto & Endo, 2015). Carboxylate groups were generated by the esterification of hydroxyl groups at the C2, 3, and 6 positions of cellulose. The carboxylate group significantly reduced the energy required to produce lignocellulose nanofibers. Inspired by these previous works, we here studied the facile mechanical disintegration of commercially available chitin powder into nanofibers by chemical treatment with maleic anhydride. Since chitin also has hydroxyl groups at the C3 and C6 positions, it would be esterified also by maleic anhydride. And generating a carboxylate group on chitin enables the facile conversion of chitin into nanofibers by the subsequent mechanical treatment.

2. Experimental

2.1. Materials

Chitin powder from crab shell with a 6.4% degree of deacetylation (DDA) was purchased from Koyo Chemical Industry (Hyogo, Japan) and used without further

purification. Maleic anhydride was purchased from Nacalai Tesque (Kyoto, Japan) and used as received.

2.2. Esterification of α-chitin with maleic anhydride

Chitin was esterified as described previously, with partial modification (Iwamoto & Endo, 2015). The scheme for preparing the esterified chitin nanofiber is shown in Fig. 1. Dry chitin powder (6 g) from crab shell reacted with maleic anhydride (30 g) at 120 ^{o}C for 3.5 hours with occasional stirring. The reactant was collected by filtration and washed with acetone and then with pure water thoroughly until the filtrate became neutral. To neutralize the introduced maleate groups, approximately 10-15 mL of 1.0 M NaOH aqueous solution was added to the esterified chitin water dispersion until the pH of the solution reached 11. The excess NaOH was then removed by washing with pure water until the pH of the suspension became 7.8. The final concentration of the esterified chitin dispersion was 1.29 wt%. The sample was stored in the refrigerator. The experimental yield was estimated by gravimetric analysis.

2.3. Mechanical disintegration

The esterified chitin was diluted with water at 0.5 wt%, and the dilution was treated with a grinder (MKCA6-3; Masuko Sangyo Co., Ltd., Kawaguchi, Japan) twice. The grinder treatment was performed at 1500 rpm with a clearance gauge of -1.5 (corresponding to a 0.15 mm shift) from the zero position, which was determined as the point of slightest contact between the grinding stones. In principle, there is no direct contact between the stones due to the presence of chitin suspension.

2.4. Film preparation

Esterified chitin nanofiber dispersion was diluted with deionized water at 0.1 wt% concentration. After removal of dissolved gases under vacuum, the aqueous dispersion was casted on Teflon plates and dried in the oven at 50 ^{o}C until the dried films detached from the plates by themselves.

2.5. Characterization

The zeta potential of aqueous esterified chitin nanofiber dispersion at 0.5 wt% was measured using a laser-Doppler method apparatus (ELSZ-1000ZS, Otsuka Electronics, Hirakata, Japan). At least five samples were measured to know the average value. For field emission scanning electron microscopic (FE-SEM) observation, esterified chitin nanofiber dispersion was diluted with an excessive amount of ethanol and dried in an oven. The dried samples were coated with an approximately 2 nm layer of platinum

using an ion sputter coater and were observed by FE-SEM (JSM-6700F; JEOL, Tokyo, Japan) operating at 2.0 kV. The light transmittances of 0.1 wt% nanofiber dispersion and the self-standing films were measured using a UV–Vis spectrophotometer (V550; JASCO, Tokyo, Japan). The degree of substitution (DS) of the maleate group introduced onto the nanofiber surface was calculated from the C and N weight percentages obtained from an elemental analyzer (Vario, EL III; Elementar, Hanau, Germany) according to:

$$C/12.01 : N/ 14.01 = (8 + 4n) : 1$$

where C and N are the weight percentages of carbon and nitrogen atoms obtained from the elemental analysis and n is the molar ratio of the DS values of the introduced maleate groups against the *N*-acetyl glucosamine unit of the nanofiber. Electrical conductivity titration method was also applied to determine DS (Fan et al., 2008a).

Infrared spectra of the samples were recorded with an FT-IR spectrophotometer (Spectrum 65, Perkin-Elmer Japan, Tokyo, Japan) equipped with an ATR attachment. The X-ray diffraction profiles were obtained using X-ray goniometer scanning from 5° to 60° with Ni-filtered Cu$K\alpha$ from an X-ray generator (Ultima IV; Rigaku, Tokyo, Japan) operating at 40 kV and 40 mA. The crystallinity indices (CI) of the samples were calculated from the ratio of the area of four crystalline peaks derived from (020), (110), (120), and (130) plane to the total area from 2 θ = 5° to 30° (Park et al., 2010). The esterified chitin crystal sizes of the (020) and (110) planes were measured from the widths at half heights of the diffraction peaks, using Scherrer's equation (Alexander, 1979).

3. Results and Discussion

3.1. Preparation of esterified chitin nanofiber

Dry α-chitin powder was reacted with neat maleic anhydride at 120 °C for 3.5 hours (Fig. 1). Although maleic anhydride is solid at room temperature, it melts above 52.6 °C, enabling a solventless reaction, which offers the advantages of low cost, ease of purification, a high reaction rate, and environmental friendliness. It is known that acid anhydride is preferentially introduced into high reactive amino group (Ifuku et al., 2011). Thus, maleyl group was at first introduced into amino group, slightly existing on chitin nanofiber in prior to hydroxyl group with lower reactivity. And then, maleic anhydride could form ester linkages with primary hydroxyl group at C6 position

preferentially due to steric hindrance, thus forming a carboxylic acid group (-COOH). After the reaction, the introduced carboxylic acid was neutralized by NaOH to change it into carboxylate salt ($-COO^-Na^+$). The esterified chitin and unmodified chitin were treated with the grinder twice to disintegrate them into nanofibers. After the mechanical treatment, the esterified chitin was homogeneously dispersed in water, and the dispersion was highly transparent compared to the unmodified chitin (Fig. 2). The regular light transmittances of esterified and unmodified chitin dispersions in water with a 0.5 wt% concentration at 600 nm were 91.5% and 13.1%, respectively. To elucidate the dispersion property of esterified chitin nanofiber in water, the dispersion was centrifuged at 10,000 rpm for 10 minutes. After the precipitate was removed, the yield of nanofibers in the supernatant fraction was 97.2% in weight. The high dispersion property comes from the surface property of the esterified chitin. The average zeta potential of the esterified chitin dispersion at pH 7.8 was -48.41 ± 9.6 mV. The high negative surface charge is obviously attributable to the carboxylate anion ($-COO^-$). The strong negative charge enabled homogeneous dispersion. Original chitin nanofiber with +54.7 ± 15.4 mV zeta potential at pH 3.0 can disperse homogeneously in acidic water. Slight amino group on the chitin enable stable dispersion of nanofiber by electrostatic repulsion. On the other hand, the chitin nanofiber precipitate in basic water immediately. Thus, esterified chitin with stable dispersion in basic water allows for the chemical reaction under basic condition or compounding with basic materials.

Figure 3a and 3b are SEM images of nanofibers obtained from esterified chitin. After two cycles of simple disk milling treatment, the esterified chitin was easily and completely disintegrated into homogeneous nanofibers over an extensive area. The average thickness and length evaluated by image analyses of 50 randomly selected nanofibers was 11.3 ± 4.4 nm and 275 ± 139 nm, respectively including a 2-nm-thick platinum coating. The disintegration efficiency of the esterified chitin was much higher than that of the unmodified chitin (Fig. 3c). Nanofibers in the unmodified chitin were thicker and heterogeneous. The thicknesses varied widely from 10 to 100 nm. The average diameter was 45 ± 8 nm. The great difference in morphology indicates that the carboxylate group of the esterified chitin helped the mechanical disintegration. Anionic charges on the fiber surface brought about interfibrillar electrostatic repulsion and osmotic pressure, facilitating mechanical disintegration. Since nanofiber is defined as a fiber with a diameter of less than 100 nm and aspect

ratio of higher than 100, the esterified material may be more nanocrystal than nanofiber.

3.2. Characterization of esterified chitin nanofibers

The degree of substitution (DS) of the maleate group of the esterified chitin nanofibers, as determined by the elemental analysis of C and N atoms, was 0.25, which means that one-fourth of the *N*-acetyl glucosamine unit was reacted with maleic anhydride. The reaction was highly reproducible. For esterification, reaction time and temperature strongly affected DS value. For example, when chitin was esterified at 100 ^{o}C for 2 hours, the DS was 0.15. The difference in DS value affected transparency of nanofiber dispersion. After the esterification, the weight of the chitin increased to 6.17 g from 6.00 g. Since the theoretical weight of the esterified chitin with 0.25 DS was 6.64 g, the percentage yield of the esterified chitin was 93% in weight. This indicates that the reaction is suitable for producing chitin nanofibers without significant mass loss during the process. Electrical conductivity titration method was also applied to determine the DS. The DS was 0.21, which was slightly lower than that from elemental analysis. The difference indicates that nanofibers were completely esterified on the surface. Moreover, inner amorphous part of nanofiber was also partially esterified.

FT-IR spectra of the esterified chitin nanofibers thus prepared are shown in Fig. 4. The amide bands at 1652 cm^{-1} and 1620 cm^{-1}, and the amide II band at 1556 cm^{-1}, are characteristics of α-chitin. In addition, the peak at 1772 cm^{-1} and the strong overlapped peak at 1556 cm^{-1} are derived from the C=O stretching vibration modes of the maleate moiety. These newly appeared absorption bands are evidence of the maleate introduced onto the nanofibers.

X-ray diffraction patterns of maleylated chitin nanofibers are shown in Fig. 5. The diffraction peaks at approximately 9.4^{o}, 19.5^{o}, 20.7^{o}, and 23.1^{o} were in good agreement with those of the typical antiparallel crystalline pattern of α-chitin, which corresponds to (020), (110), (120), and (130) planes, respectively (Minke & Blackwell, 1978). The relative crystallinity of esterified chitin nanofibers estimated from the comparison between crystalline and total diffraction areas was 74%, which is slightly higher than unmodified chitin (68%). The slight increase in the relative crystallinity of chitin nanofiber may be attributed to the removal of amorphous part. Maleic anhydride preferentially reacted with amorphous region and esterified

amorphous was removed by washing process. Moreover, maleate groups were introduced onto the surface and the amorphous part of the nanofibers, and that the original chitin crystalline structure was maintained after the esterification reaction. The crystal sizes of the esterified nanofibers estimated by XRD patterns were 6.8 nm and 5.4 nm at (020) and (110) planes, respectively.

We prepared a cast film using the maleated chitin nanofiber dispersion. The cast film had a much higher transparency than that from the unmodified chitin nanofiber (Fig. 6). The regular light transmittances of the esterified and unmodified chitin nanofiber films at 600 nm were 74.4% and 2.4%, respectively. The significant difference in transparency is due to the differences in dispersibility in water and nanofiber thickness between the two kinds of nanofibers. That is, esterified nanofibers that were narrower and more dispersible in water were slowly concentrated by the evaporation of the water so that nanofibers were piled up uniformly and gradually. The nanofibers were so densely stacked that cavities in the cast film were almost completely removed. Since the cast film was free from light scattering in the sheet, it became transparent (Nogi et al., 2009).

4. Conclusion

Esterified chitin nanofibers with 0.25 DS were successfully prepared by the reaction of chitin in neat maleic anhydride and subsequent mechanical disintegration without losing its crystalline structure. The esterification significantly facilitated the mechanical disintegration due to the strong electrostatic repulsion and osmotic pressure. The surface carboxylate group enhanced the nanofibers' homogeneous dispersion property in water at higher pH, which enabled us to obtain a highly transparent film by a casting method. We expect that chitin nanofibers with an anionic hydrophilic functional group, a uniform nanofiber morphology, and a very high surface ratio will be available as a novel nano-biomaterial that can function in a variety of applications.

References

Alexander, L. E. (1979). X-ray diffraction methods in polymer science. Ed. Krieger, A. R., Huntington, New York.

234 Chen, P.-Y., Lin, A. Y.-M., McKittrick, J., & Meyers, M. A. (2008). Structure and
235 mechanical properties of crab exoskeletons. *Acta Biomaterialia*, *4*, 587–596.
236 Dutta, A. K., Yamada, K., Izawa, H., Morimoto, M., Saimoto, H., & Ifuku, S. (2013).
237 Preparation of chitin nanofibers from dry chitin powder by star burst system:
238 dependence on number of passes. *Journal of Chitin and Chitosan Science*, *1*, 59–64.
239 Fan, Y., Saito, T., & Isogai, A. (2008a). Chitin nanocrystals prepared by TEMPO-
240 mediated oxidation of *α*-chitin. *Biomacromolecules*, *9*, 192–198.
241 Fan, Y., Saito, T., & Isogai, A. (2008b). Preparation of chitin nanofibers from squid
242 pen *β*-chitin by simple mechanical treatment under acid conditions.
243 *Biomacromolecules*, *9*, 1919–1923.
244 Fan, Y., Fukuzumi, H. Saito, T., & Isogai, A. (2012). Comparative characterization of
245 aqueous dispersions and cast films of different chitin nanowhiskers/nanofibers,
246 *International Journal of Biological Macromolecules*, *50*, 69–76.
247 Ifuku, S., Nogi, M., Abe, K., Yoshioka, M., Morimoto, M., Saimoto, H., & Yano, H.
248 (2009). Preparation of chitin nanofibers with a uniform width as *α*-chitin from crab
249 shells. *Biomacromolecules*, *10*, 1584–1588.
250 Ifuku, S., Nogi, M., Yoshioka, M., Morimoto, M., Yano, H., & Saimoto, H. (2010).
251 Fibrillation of dried chitin into 10‐20 nm nanofibers by a simple grinding method
252 under acidic conditions. *Carbohydrate Polymers*, *81*, 134–139.
253 Ifuku, S., Nogi, M., Abe, K., Yoshioka, M., Morimoto, M., Saimoto, H., & Yano, H.
254 (2011). Simple preparation method of chitin nanofibers with a uniform width of 10–
255 20nm from prawn shell under neutral conditions. *Carbohydrate Polymers*, *84*, 762–
256 764.
257 Ifuku, S., Miwa, T., Morimoto, M., & Saimoto, H. (2011). Preparation of highly
258 chemoselective *N*-phthaloyl chitosan in aqueous media. *Green Chemistry*, *13*, 1499–
259 1502.
260 Ifuku, S., Yamada, K., Morimoto, M., & Saimoto, H. (2012). Nanofibrillation of dry
261 chitin powder by Star Burst system. *Journal of Nanomaterials*, *2012*, 1–7.
262 Iwamoto, S., & Endo, T. (2015). 3 nm Thick lignocellulose nanofibers obtained from
263 esterified wood with maleic anhydride. *ACS Macro Lett*., *4*, 80-83.
264 Kose, R., & Kondo, T. (2011). Favorable 3D-network formation of chitin nanofibers
265 dispersed in water prepared using aqueous counter collision. *Sen-I Gakkaishi*, *67*, 91–
266 95.

Lu, Y., Sun, Q., She, X., Xia, Y., Liu, Y., Li, J., & Yang, D. (2013). Fabrication and characterisation of α-chitin nanofibers and highly transparent chitin films by pulsed ultrasonication. *Carbohydrate Polymers*, *98*, 1497-1504.

Minke, R. & Blackwell, J. (1978). The structure of *a*-chitin. *Journal of Molecular Biology*, *120*, 167–181.

Mushi, N. E., Butchosa, N., Salajkova, M., Zhou, Q., & Berglund, L. A. (2014). Nanostructured membranes based on native chitin nanofibers prepared by mild process. *Carbohydrate Polymers*, *112*, 255-263.

Mushi, N. E., Kochumalayil, J., Cervin, N. T., Zhou, Q., & Berglund, L. A. (2016). Nanostructurally Controlled Hydrogel Based on Small-Diameter Native Chitin Nanofibers: Preparation, Structure, and Properties. *ChemSusChem*, *9*, 989–995.

Nogi, M., Iwamoto, S., Nakagaito, A. N., & Yano, H. (2009). Optically transparent nanofiber paper. *Advanced Materials*, *21*, 1595-1598.

Park, S., Baker, J. O., Himmel, M. E., Parilla, P. A., & Johnson, D. K. (2010). Cellulose crystallinity index: Measurement techniques and their impact on interpreting cellulase performance. *Biotechnology for Biofuels*, *3*, 1–10.

Raabe, D., Romano, P., Sachs, C., Fabritius, H., Al-Sawalmih, A., Yi, S.-B., Servos, G., & Hartwig, H. G. (2006). Microstructure and crystallographic texture of the chitin–protein network in the biological composite material of the exoskeleton of the lobster *Homarus americanus*. *Material Science and Engineering: A*, *421*, 143–153.

Figure Captions

Fig. 1. Preparation scheme for the surface-maleated chitin nanofiber

Fig. 2. Photograph and UV-Vis spectra of (a) untreated and (b) maleated chitin nanofiber dispersions

Fig. 3. SEM images of (a and b) esterified and (c) unmodified chitin nanofiber. Scale bar: (a) 1000 nm, (b and c) 200 nm.

Fig. 4. FT-IR spectra of (a) unmodified and (b) maleated chitin nanofibers

Fig. 5. X-ray diffraction profiles of (a) unmodified and (b) maleated chitin nanofibers

Fig. 6. Appearances, SEM images, and UV-Vis spectra of (a) maleated and (b) unmodified chitin nanofiber film. Scale bar: 200 nm

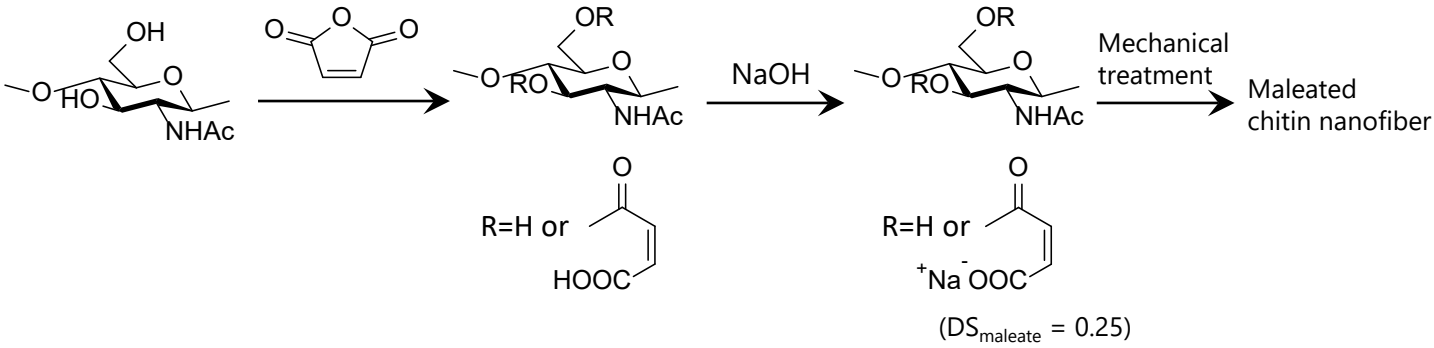

Fig. 1. Preparation scheme for the surface maleated chitin nanofiber

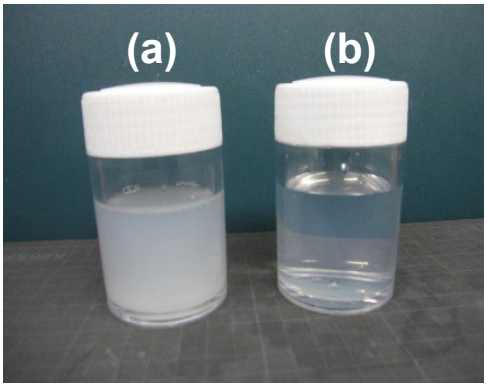

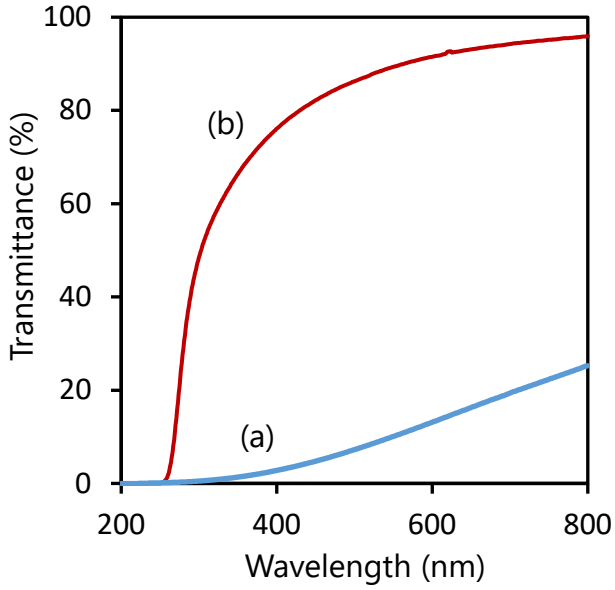

Fig. 2. Photograph and UV-Vis spectra of (a) untreated and (b) maleated chitin nanofiber dispersion

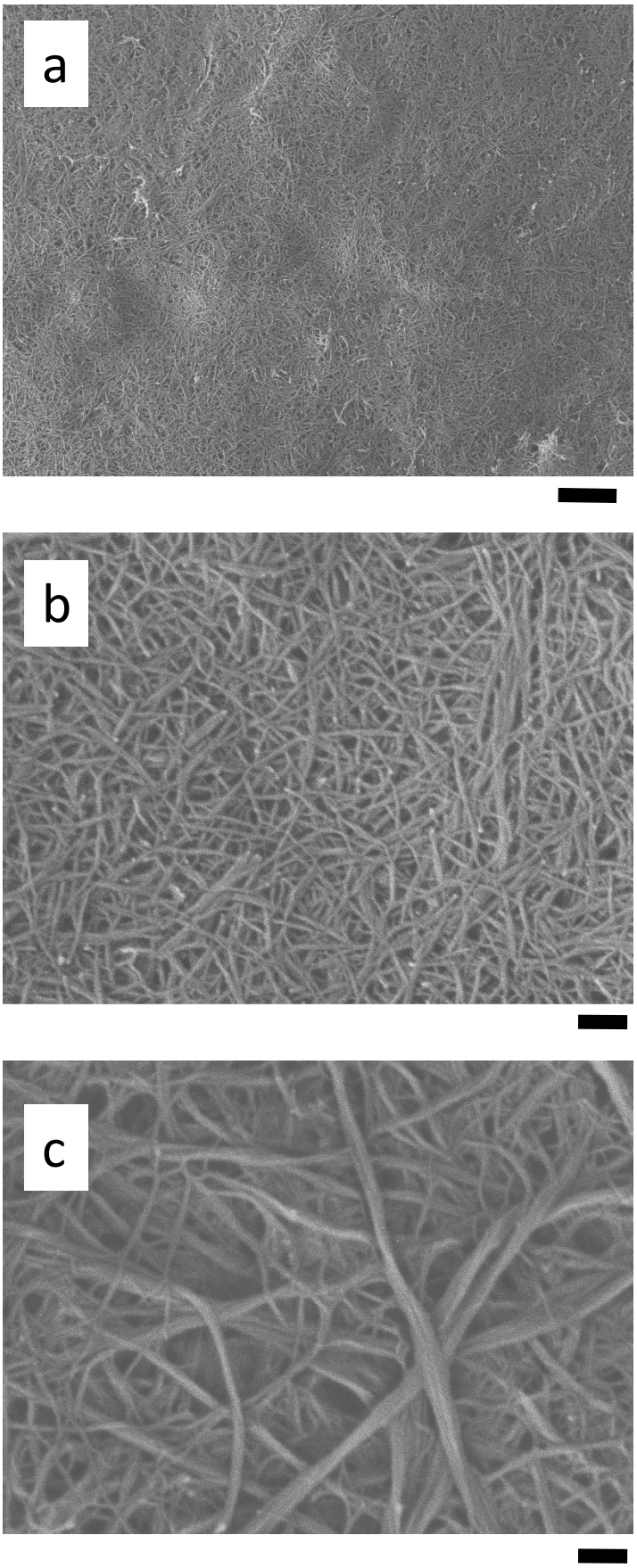

Fig. 3. SEM images of (a and b) esterified and (c) unmodified chitin nanofiber. Scale bar: (a) 1000 nm, (b and c) 200 nm.

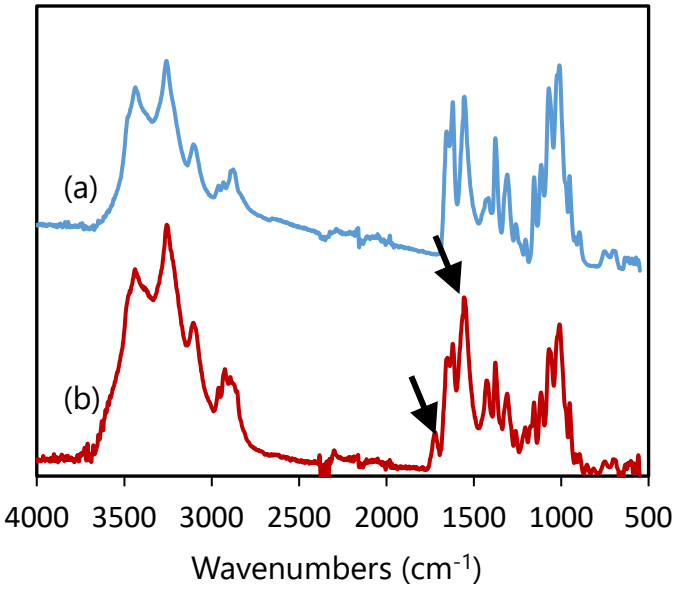

Fig. 4. FT-IR spectra of (a) unmodified and the (b) maleated chitin nanofiber

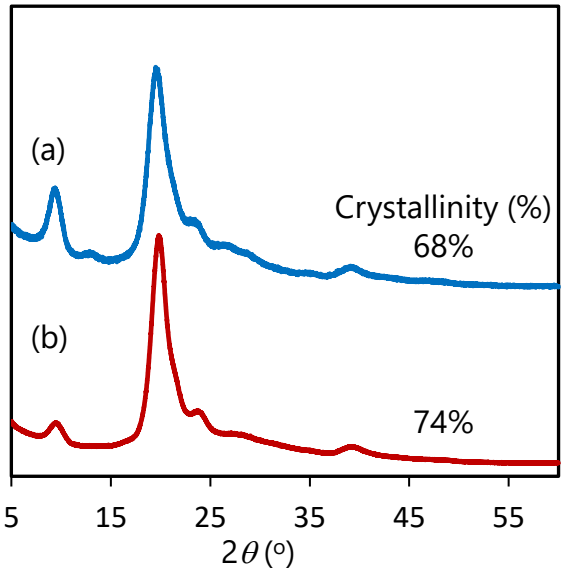

Fig. 5. X-ray diffraction profiles of (a) unmodified and the (b) maleated chitin nanofibers

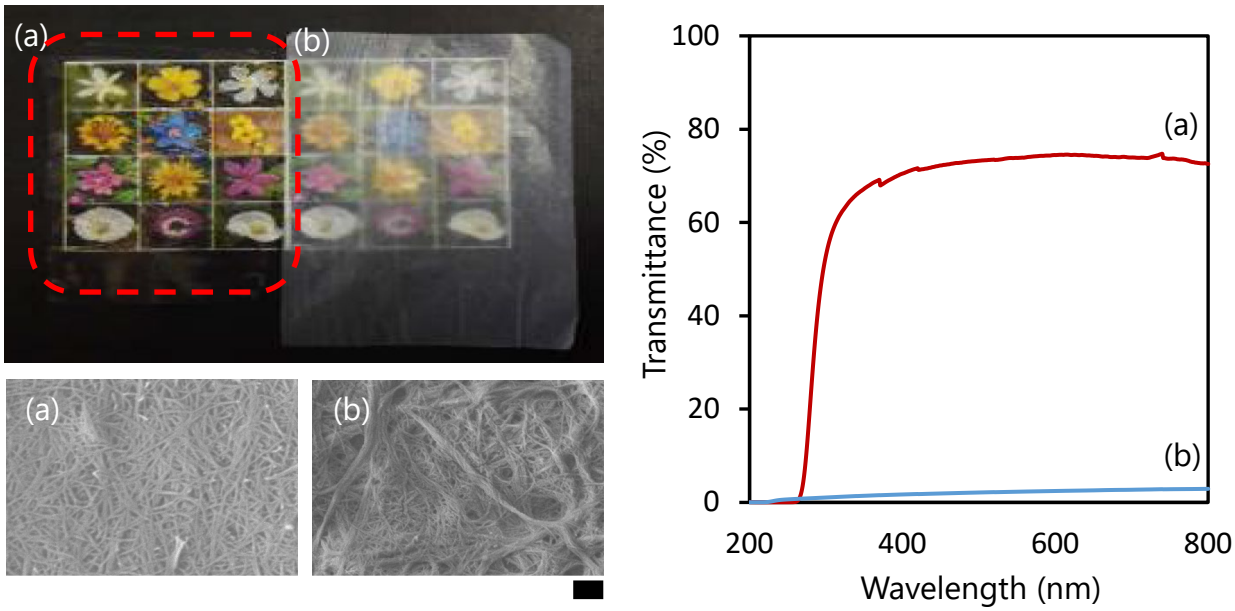

Fig. 6. Appearances, SEM images, and UV-Vis spectra of (a) maleated and (b) unmodified chitin nanofiber film